AIP | The Journal of Chemical Physics

Line coupling effects in the isotropic Raman spectra of N2: A quantum calculation at room temperature

Franck Thibault, Christian Boulet, and Qiancheng Ma

Citation: The Journal of Chemical Physics **140**, 044303 (2014); doi: 10.1063/1.4862082
View online: http://dx.doi.org/10.1063/1.4862082
View Table of Contents: http://scitation.aip.org/content/aip/journal/jcp/140/4?ver=pdfcov
Published by the AIP Publishing

Line coupling effects in the isotropic Raman spectra of N_2: A quantum calculation at room temperature

Franck Thibault,[1,a)] Christian Boulet,[2] and Qiancheng Ma[3]
[1]*Institut de Physique de Rennes, UMR CNRS 6251, Université de Rennes I, Campus de Beaulieu, Bât. 11B, F-35042 Rennes, France*
[2]*Institut des Sciences Moléculaires d'Orsay, UMR CNRS 8214, Université Paris-Sud 11, Campus d'Orsay, Bât. 350, F-91405 Orsay, France*
[3]*NASA/Goddard Institute for Space Studies and Department of Applied Physics and Applied Mathematics, Columbia University 2880 Broadway, New York, New York 10025, USA*

(Received 18 October 2013; accepted 2 January 2014; published online 23 January 2014)

We present quantum calculations of the relaxation matrix for the Q branch of N_2 at room temperature using a recently proposed N_2-N_2 rigid rotor potential. Close coupling calculations were complemented by coupled states studies at high energies and provide about 10 200 two-body state-to state cross sections from which the needed one-body cross-sections may be obtained. For such temperatures, convergence has to be thoroughly analyzed since such conditions are close to the limit of current computational feasibility. This has been done using complementary calculations based on the energy corrected sudden formalism. Agreement of these quantum predictions with experimental data is good, but the main goal of this work is to provide a benchmark relaxation matrix for testing more approximate methods which remain of a great utility for complex molecular systems at room (and higher) temperatures. © *2014 AIP Publishing LLC*. [http://dx.doi.org/10.1063/1.4862082]

I. INTRODUCTION

Collision-induced rotational energy transfer in molecular gases plays an important role in a variety of gas phase processes, such as pressure broadening and shifting and/or mixing of spectral lines.[1] The most accurate calculation of the corresponding cross-sections involves solving sets of coupled differential equations using the close coupling (CC) method.[2] However, even with present day computers, such calculations remain prohibitively expensive for complex molecular systems (e.g., a mixture of polyatomic molecules). As a result of these limitations, various approximate models have been developed. They include fitting laws and more accurate scaling approaches; amongst the latter, those derived from the energy corrected sudden approximation (ECS) seem to be very powerful.[1] Alternatively, some researchers have developed purely classical[3] or semi-classical[4,5] calculations of the corresponding relaxation matrices.

In a recent paper,[6] some of us have shown that it is possible to introduce line coupling effects within the semi-classical Robert-Bonamy formalism,[7] leading to a new method for calculating the off-diagonal elements of the relaxation matrix. We have also shown in that paper that considering line coupling leads to better agreement between semi-classical and fully quantum linewidths (diagonal elements of the relaxation matrix W), starting from the same intermolecular potential for the N_2-N_2 pair. That system was chosen for benchmarking purposes: Thibault *et al.*[8,9] had previously reported detailed fully quantum calculations of the half-widths of the isotropic Raman Q lines, based on a very recent potential energy surface (PES) proposed by Gomez *et al.*[10] Before investigating the validity of this new semi-classical approach for the calculation of the off-diagonal elements of W, it is necessary to dispose of fully quantum non-diagonal elements which will be used as a reference for testing the semi-classical results. Such CC calculations were previously reported by Green and Huo,[11] but based on the PES of van der Avoird,[12] which has been shown to need some refinements.[8,9,13] More recently, Fonfria *et al.*[14] have reported CC two-body cross-sections at total energies too low to obtain converged results for temperatures higher than 50 K. It is therefore necessary to considerably extend these calculations in order to work at room temperature. This is the purpose of the present paper; the comparison with the semi-classical results obtained from the method of Ref. 6 will be presented in a forthcoming paper.

In Sec. II, an outline of the quantum formalism and numerical calculations is given together with a brief summary of the ECS formalism. Section III compares the current results with experimental data and previous calculations and provides a brief discussion of the convergence of the calculations, before a brief summary of our findings.

II. THEORY

A. Some definitions

Within the impact and binary collisions approximations, the effects of molecular collisions on isotropic Raman spectra is described by a relaxation matrix $W(j'_1, j_1; T)$ whose rows and columns are labeled by spectral lines[1,15,16] (for simplicity, j_1 means here $Q(j_1)$; j_1 and j'_1 refer to the spectrally active molecule). At low pressures, only diagonal elements are important since they define the half-widths of non-overlapping lines ($\gamma(j, T) \equiv W(j, j; T)$). At higher pressures, off-diagonal elements become important and

a)Author to whom correspondence should be addressed. Electronic mail: franck.thibault@univ-rennes1.fr

describe line mixing transfer of intensity between overlapping lines. When the PES does not contain any vibrational dependence, W is real and may be written in terms of one-body cross-sections which are, for off-diagonal elements, the negative of ordinary state-to-state cross-sections for rotational excitation (or deexcitation):

$$W(j_1', j_1; T) = \frac{n_2 \bar{v}}{2\pi c}\sigma^0(j_1', j_1; T) = -\frac{n_2 \bar{v}}{2\pi c}\sigma(j_1 \rightarrow j_1'; T), \quad (1)$$

where n_2 is the perturber density and $\bar{v}$ is the mean relative velocity. These cross-sections may be written as a weighted sum of two body rotational state to state cross-sections:

$$\sigma(j_1 \rightarrow j_1'; T) = \sum_{j_2} \rho(j_2) \sum_{j_2'} \sigma(j_1, j_2 \rightarrow j_1', j_2'; T), \quad (2)$$

where j_2 and j'_2 refer to the bath molecule and $\rho(j_2)$ is the normalized rotational population of level j_2 (including the spin factor). Finally, we recall that the two-body cross-sections, at a given temperature T, are obtained as a thermal average over the initial relative kinetic energy $E_{\rm kin}$ of inelastic cross-sections $\sigma(j_1, j_2 \rightarrow j'_1, j'_2; E_{kin})$:

$$\sigma(j_1, j_2 \rightarrow j_1', j_2'; T) = \frac{1}{(k_B T)^2}\int_{E_s}^{\infty} \sigma(j_1, j_2 \rightarrow j_1', j_2'; E_{kin}) \times \exp(-E_{kin}/k_B T) E_{kin} dE_{kin}, \quad (3)$$

where $E_{\rm S}$ is the minimum kinetic energy for the levels j'_1 and j'_2 to become accessible.

In cases where the collision dynamics do not depend on vibrational motion, a sum rule exists which says that, for each line, the diagonal elements of W are equal to the negative of the sum of the off-diagonal elements:[16]

$$\sum_{j_1'} W(j_1', j_1; T) = 0, \quad (4a)$$

or

$$\sum_{j_1' \neq j_1} \sigma(j_1 \rightarrow j_1'; T) = \sigma^0(j_1, j_1; T). \quad (4b)$$

Another important relation is the detailed balance relationship:

$$\rho(j_1)\sigma(j_1 \rightarrow j_1'; T) = \rho(j_1')\sigma(j_1' \rightarrow j_1; T), \quad (5)$$

which results, at a more elementary level, from the detailed balance for the two-body cross-sections:

$$\rho(j_1)\rho(j_2)\sigma(j_1, j_2 \rightarrow j_1', j_2'; T) = \rho(j_1')\rho(j_2')\sigma(j_1', j_2' \rightarrow j_1, j_2; T), \quad (6)$$

the latter resulting from the microscopic reversibility, at a more elementary level:

$$(2j_1+1)(2j_2+1)E_k\sigma(j_1, j_2 \rightarrow j_1', j_2'; E_k) = (2j_1'+1)(2j_2'+1)(E_k+E(j_1)-E(j_1')+E(j_2)-E(j_2')) \times \sigma(j_1', j_2' \rightarrow j_1, j_2; E_k+E(j_1)-E(j_1')+E(j_2)-E(j_2')). \quad (7)$$

B. Quantum dynamical calculations

Quantum dynamical calculations were performed on the four dimensional ab initio potential energy surface of Ref. 10 determined by using symmetry adapted perturbation theory. This interaction potential, between rigid rotors, is expected to be the most accurate to date.[8–10,17] In particular, it provides accurate self-broadening coefficients over a wide range of temperatures (77–1700 K) for Raman isotropic Q lines.[8,9]

Close-coupling and coupled states calculations were performed with the MOLSCAT code and its parallel version.[18] Technical details handling the PES and the dynamical calculations can be found in Refs. 8 and 9. Both variants of N_2 have been considered, ortho (oN_2; even $j's$) and para (pN_2; odd $j's$). The PES does not allow interconversion between ortho and para species. Following previous work,[11,14,16] the calculations were performed assuming that the two colliding molecules are distinguishable, even for oN_2-oN_2 or pN_2-pN_2 collisions, thus neglecting (small) resonance-exchange effects. Moreover, since the experimental results we are comparing with[19] involve vibrational excitation of one of the two N_2 molecules, such a contribution will be much smaller than in the case of two molecules in the same vibrational state. Dynamical calculations were performed at various total energies E_T, and thus at various kinetic energies $E_{kin} = E_T - E_{rot}(j_1, j_2)$ for a given total internal rotational energy given by $E_{rot}(j_1, j_2) = Bj_1(j_1+1) + Bj_2(j_2+1)$ with the rotational constant $B = 1.998\ \text{cm}^{-1}$. Here we only present results for an ortho active molecule (j_1, j'_1 even).

Two-body state-to-state cross-sections $\sigma(j_1 j_2 \rightarrow j'_1 j'_2; E_{kin})$ for ortho–para nitrogen collisions were calculated using the CC method over a grid of 150 total energies up to 450 cm^{-1}, thus including the (asymptotically) open two-body rotational energy levels lower than $E_{rot}(6, 13) = 447.6\ \text{cm}^{-1}$, and completed by 15 coupled states calculations for total energies between 500 and 1500 cm^{-1} (thus including the open two-body rotational levels up to $j_1 = 22, j_2 = 15$). Therefore two-body rate constants (see below) involving rotational energy levels lower than $E_{rot}(6, 13)$ are CC/CS (coupled states) results while results for rotational energy levels higher are fully CS.

Similarly, calculations for oN_2-oN_2 were performed using the CC method over a grid of 254 total energies up to 505 cm^{-1}, including the open two-body rotational energy levels lower than $E_{rot}(6, 14) = 503.55\ \text{cm}^{-1}$, and completed by 15 coupled states calculations up to 1500 cm^{-1} (including two-body rotational levels up to $j_1 = 24, j_2 = 12$). Therefore two-body rate constants for rotational energy levels lower than $E_{rot}(6, 14)$ are CC/CS results while results for rotational energy levels higher are fully CS. In order to illustrate the progress of the computational power, note that the CC calculations of Ref. 11 were limited to total energies up to 200 cm^{-1} while CS calculations were obtained up to 700 cm^{-1}.

Because of the limitations of our grid in kinetic energies, for oN_2-pN_2 and oN_2-oN_2 we have only retained the cross-sections $\sigma(j_1 j_2 \rightarrow j'_1 j'_2; T)$, respectively, between the very first 70 two-body rotational levels (i.e., up to $j_1 = 10, j_2 = 15$ associated with a rotational energy of about 700 cm^{-1}) and those between the very first

75 two-body rotational levels (i.e., up to $j_1 = 2, j_2 = 18$ associated with a rotational energy of about 695 cm^{-1}). However experiments measure effective one particle cross sections[14,19] $\sigma(j_1 \rightarrow j'_1; T)$ that are obtained from Eq. (2). In evaluating this double sum, it is necessary to include all the significantly populated bath level j_2, as well as all the significant two-body cross sections (i.e., those with a small inelasticity). The most populated level at 300 K corresponds to $j \approx 6$–8. We include all the levels up to $j_2 = 18$, which corresponds to 98% of the population and the sum over j'_2 incorporates contributions up to $j'_2 = j_2 + 20$. Therefore, due to the limits of our CC/CS calculations, it was necessary to check the convergence of our CC/CS one body cross-sections. We have therefore developed a method inspired by the previous work of Green and Huo:[11] we have used the ECS formalism to generate, when necessary, extrapolated two-body cross-sections (i.e., those not obtained from our CC/CS calculations). If the ECS contribution to Eq. (2) remains small, then the one body cross-section may be reasonably considered as a CC/CS result; otherwise it will not be retained as a reference value. It is therefore necessary to recall briefly some basic ECS relations allowing the calculation of all the two body state to state cross sections from a limited set of "fundamental" ones:

$$Q(L_1, L_2) \equiv \sigma(L_1, L_2 \rightarrow 0, 0; T). \tag{8}$$

Note here that our definition of these basic cross-sections is different from that of Green and Huo[11,16] who used $Q^{GH}(L_1, L_2) \equiv \sigma(0, 0 \rightarrow L_1, L_2)$, so that the two sets are related by the detailed balance Eq. (6).

C. ECS formalism

Within the approach of Green,[16] a non-diagonal two-body cross-section can be deduced from the following scaling relation:

$$\sigma(j_1, j_2 \rightarrow j'_1, j'_2; T) = (2j'_1 + 1)(2j'_2 + 1) \sum_{L_1, L_2} (2L_1 + 1)(2L_2 + 1) \begin{pmatrix} j_1 & L_1 & j'_1 \\ 0 & 0 & 0 \end{pmatrix}^2 \begin{pmatrix} j_2 & L_2 & j'_2 \\ 0 & 0 & 0 \end{pmatrix}^2 \times \left[\frac{24 + (\Omega(L_1, L_2)\tau_c)^2}{24 + (\Omega(j_1, j_2)\tau_c)^2} \right]^2 Q(L_1, L_2), \tag{9}$$

where $\begin{pmatrix} \cdots \end{pmatrix}$ is a 3j-symbol. Eq. (9) is applied only for energetically downward collisions (positive transfer from rotation to translation) while upward cross-sections are obtained from detailed balance (Eq. (6)). According to De Pristo *et al.*,[20] the adiabaticity factor $[\frac{24+(\Omega(L_1,L_2)\tau_c)^2}{24+(\Omega(j_1,j_2)\tau_c)^2}]^2$ which accounts for the non-resonant character of the collisions is defined in terms of an average collision duration $\tau_c = l_c/\bar{v}$ where l_c is an adjustable scaling length. The frequency factor represents the dominant inelasticity for level j_1,j_2 and it can be defined in various ways. Following the previous analysis of Green,[16] we used:

$$\Omega(j_1, j_2) = 2B(j_1 + j_2). \tag{10}$$

III. RESULTS AND DISCUSSION

In the following, results will be indifferently presented as relaxation matrix elements $W_{j',j}$ in units of 10^{-3} cm^{-1} atm^{-1} (Eq. (1)) or as one body excitation rates $n_2\bar{v}\sigma(j_1 \rightarrow j'_1; T)$, in units of μs^{-1} $Torr^{-1}$ which were adopted by Sitz and Farrow[19] to present their experimental data.

A. Determination of the ECS scaling length

As may be seen from Eq. (8), the basic $Q(L_1, L_2)$ are also given by the CC/CS calculations since they simply correspond to the usual inelastic cross-sections. They are available up to $(L_1 = 18; L_2 = 18)$ and are given in Table I. Therefore the next step is the determination of the only unknown parameter: l_c. This was determined via a least-square fit of Eq. (9) to the complete set of 10 232 available CC/CS cross-sections. The best fit was obtained for $l_c = 2.4$ Å. Among the 10 232 cross sections, 72% of the ECS predictions were in error by less than a factor of 2, with a root mean square relative error of 0.12; 28% were in error by more, with an extremely large rms relative error of 2.3, reflecting very large errors in a very small number of tiny cross-sections, mostly corresponding to very large inelasticity.

Before continuing, it is worthwhile comparing these results with those previously obtained by Huo and Green (LSQ method in Ref. 11a)) with a slightly different procedure : they fitted both the scaling length *and* the fundamental $Q^{GH}(L_1, L_2)$ rates, while we keep these fixed to the CC/CS values. They obtained a scaling length of 2.5 Å, very close to our value. Now, by comparing the last column of Table I, to the basic $\sigma_{LSQ}(0, 0 \rightarrow L_1, L_2)$ determined by Huo and Green (column labeled LSQ in Table III of Ref. 11a)) it appears that their $\sigma_{LSQ}(0, 0 \rightarrow L_1, L_2)$ are close to our CC/CS values (deduced from the $Q(L_1, L_2)$, via the detailed balance), at least for the lowest (L_1,L_2) couples. It is therefore not surprising that the two methods converge towards very similar solutions for the effective one-body rate constants.

B. Determination of the $\sigma(j_1 \rightarrow j'_1; T)$ cross-sections

On this basis it was possible to calculate one body cross-sections in different ways, from Eq. (2). Some results are given in Table II. Results labeled CC/CS used only *available* CC/CS two body cross-sections, setting all missing ones to zero. Results labeled ECS correspond to the same sum except that we used ECS two body cross-sections. Comparison of these two columns gives an idea of the accuracy of the ECS predictions for the (highly averaged) one body cross-sections. The third column gives an ECS estimation of the missing CC/CS terms in the double sum of Eq. (2) (those set to zero). Finally, the CC/CS results were supplemented by adding the ECS correction to the CC/CS results, leading to the final results (last column).

When the ECS correction is much smaller than the pure CC/CS contribution (less than about a few per cent), the final result may be considered as a confident result: "quite a pure CC/CS cross-section." This is the case for the $\sigma(j_1 = 4 \rightarrow j'_1; T = 298\,K)$ cross-sections appearing in Table II(a).

TABLE I. Basic rates for N_2-N_2 treated as distinguishable particles at 298 K, in μs^{-1} $Torr^{-1}$. Column (1) corresponds to the $\sigma(L_1, L_2 \rightarrow 00)$ as given by our CC/CS calculations. Column (2) gives the corresponding $\sigma(00 \rightarrow L_1, L_2)$ obtained from column (1) via the detailed balance (Eq. (6)). To be compared with column labeled LSQ in Table III of Ref. 11(a).

L_1	L_2	(1)	(2)
0	2	4.26×10^{-1}	2.011
0	4	6.14×10^{-2}	0.456
0	6	2.4×10^{-2}	0.208
0	8	1.182×10^{-2}	0.1
0	10	6.39×10^{-3}	4.67×10^{-2}
0	12	3.98×10^{-3}	2.22×10^{-2}
0	14	2.42×10^{-3}	9.35×10^{-3}
0	16	1.32×10^{-3}	3.2×10^{-3}
0	18	6.79×10^{-4}	9.4×10^{-4}
2	2	1.65×10^{-1}	3.673
2	4	3.651×10^{-2}	1.28
2	6	1.11×10^{-2}	0.456
2	8	5.4×10^{-3}	0.217
2	10	2.72×10^{-3}	9.38×10^{-2}
2	12	1.55×10^{-3}	4.09×10^{-2}
2	14	8.49×10^{-4}	1.55×10^{-2}
2	16	4.46×10^{-4}	5.09×10^{-3}
2	18	2.24×10^{-4}	1.46×10^{-3}
4	4	2.324×10^{-2}	1.282
4	6	8.51×10^{-3}	5.49×10^{-1}
4	8	3.52×10^{-3}	2.23×10^{-1}
4	10	2.09×10^{-3}	1.13×10^{-1}
4	12	1.074×10^{-3}	4.454×10^{-2}
4	14	5.72×10^{-4}	1.64×10^{-2}
4	16	3.02×10^{-4}	5.42×10^{-3}
4	18	1.58×10^{-4}	1.62×10^{-3}
6	6	8.14×10^{-3}	6.14×10^{-1}
6	8	3.84×10^{-3}	2.84×10^{-1}
6	10	1.45×10^{-3}	9.22×10^{-2}
6	12	7.11×10^{-4}	3.45×10^{-2}
6	14	3.59×10^{-4}	1.2×10^{-2}
6	16	1.94×10^{-4}	4.07×10^{-3}
6	18	9.64×10^{-5}	1.16×10^{-3}
8	8	3.464×10^{-3}	2.51×10^{-1}
8	10	1.185×10^{-3}	7.365×10^{-2}
8	12	3.7×10^{-4}	1.76×10^{-2}
8	14	2.29×10^{-4}	7.52×10^{-3}
8	16	1.154×10^{-4}	2.38×10^{-3}
8	18	5.82×10^{-5}	6.86×10^{-4}
10	10	9.19×10^{-4}	4.9×10^{-2}
10	12	2.76×10^{-4}	1.125×10^{-2}
10	14	1.04×10^{-4}	2.92×10^{-3}
10	16	5.29×10^{-5}	9.34×10^{-4}
10	18	3.57×10^{-5}	3.61×10^{-4}
12	12	2.76×10^{-4}	8.61×10^{-3}
12	14	7.4×10^{-5}	1.6×10^{-3}
12	16	4.48×10^{-5}	6.05×10^{-4}
12	18	2.14×10^{-5}	1.66×10^{-4}
14	14	2.125×10^{-5}	3.16×10^{-4}
14	16	1.86×10^{-5}	1.74×10^{-4}
14	18	1.3×10^{-5}	6.93×10^{-5}
16	16	1.71×10^{-5}	1.0×10^{-4}
16	18	7.9×10^{-6}	2.64×10^{-5}
18	18	4.8×10^{-6}	9.21×10^{-6}

TABLE II. One body rate constants for $j_1 \rightarrow j'_1$ transitions at 298 K, in 10^{-3} cm^{-1} atm^{-1}, calculated from Eq. (2). Column labeled CC/CS: sum of the available CC/CS two body rates. Column labeled Equivalent ECS: sum of the same two body rates but obtained from the ECS scaling relation (Eq. (9)). Column labeled ECS complement: sum of the two body rates missing in the CC/CS calculation and calculated from the ECS scaling relation. Final result corresponds to column (2) + column (4).

j'_1	CC/CS	Equivalent ECS	ECS complement	Final result
		(a) For $j_1 = 4$		
0	2.02	1.88	0.04	2.06
2	11.43	10.34	0.18	11.61
6	14.85	12.0	0.24	15.09
8	8.37	6.17	0.18	8.55
10	4.5	3.3	0.15	4.65
12	2.12	1.54	0.12	2.24
14	0.8	0.58	0.083	0.883
16	0.2	0.17	0.05	0.25
18	0.008	0.045	0.037	0.045
		(b) For $j_1 = 14$		
0	0.168	0.098	0.016	0.184
2	0.873	0.55	0.09	0.963
4	1.55	1.11	0.18	1.73
6	2.3	1.79	0.26	2.56
8	3.21	2.54	0.35	3.56
10	5.0	3.34	0.47	5.47
12	10.6	4.93	0.74	11.34
16	3.13	2.78	0.81	...
18	0.1	0.99	0.79	...

First note the very good accuracy of the ECS predictions for small inelasticities. Consider for instance the case $j_1 = 4 \rightarrow j'_1 = 6$ and the sum $\sum_{j'_2} \sigma\left(j_1 = 4, j_2 \rightarrow j'_1 = 6, j'_2; T\right)$ plotted as function of j_2 in Fig. 1(a). As it appears the most important differences between CC/CS and ECS results appear mainly for high j_2 values which are weighted by small populations in Eq. (2). Consequently, as shown in Fig. 2(a), the two calculations of Eq. (2) lead to values differing only by 20%. One may also observe the good convergence of the CC/CS sum.

Things are more complex for higher j_1 values, as may be seen from Table II(b), which corresponds to $j_1 = 14$. As expected, the accuracy of the ECS predictions is not as good for such a high j_1 value. Moreover, while the ECS supplement remains small (when compared to the CC/CS sum) up to $j'_1 = 12$, it becomes important for $j'_1 = 16 - 18$ (and higher j'_1) and is probably underestimated. This may be easily understood from a similar analysis as above. We consider the case $j_1 = 14 \rightarrow j'_1 = 16$. As shown in Fig. 1(b) important differences exist for the sum $\sum_{j'_2} \sigma\left(j_1 = 14, j_2 \rightarrow j'_1 = 16, j'_2; T\right)$ calculated by CC/CS or ECS methods. The convergence of the summation (Eq. (2)) over j_2 values is shown in Fig. 2(b). The CC/CS and ECS calculations start to diverge for $j_2 \geq 8$ but that divergence stops abruptly for $j_2 \geq 12$ due to the lack of CC/CS values. Therefore an important ECS complement is needed in that case as it appears in Table II(b). Hence $\sigma(j_1 = 14 \rightarrow j'_1 > 14;\ T = 298\,\mathrm{K})$ cannot be considered as

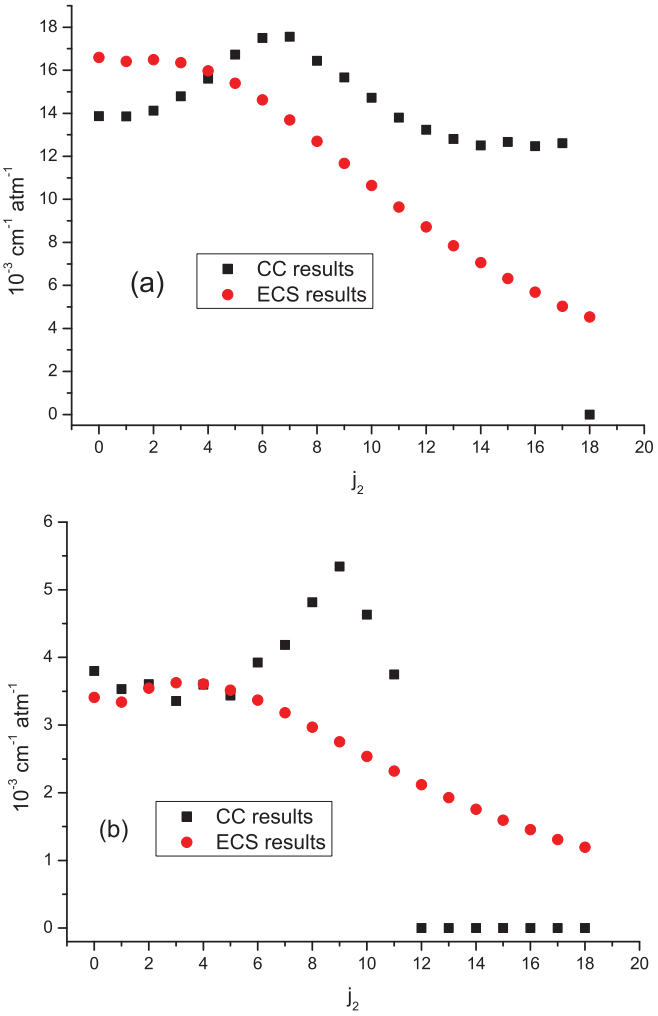

FIG. 1. $\sum_{j'_2} \sigma\left(j_1, j_2 \rightarrow j'_1, j'_2; T\right)$ (in 10^{-3} cm^{-1} atm^{-1}) as function of j_2: (a) for $j_1 = 4$; $j'_1 = 6$ and (b) for $j_1 = 14$; $j'_1 = 16$.

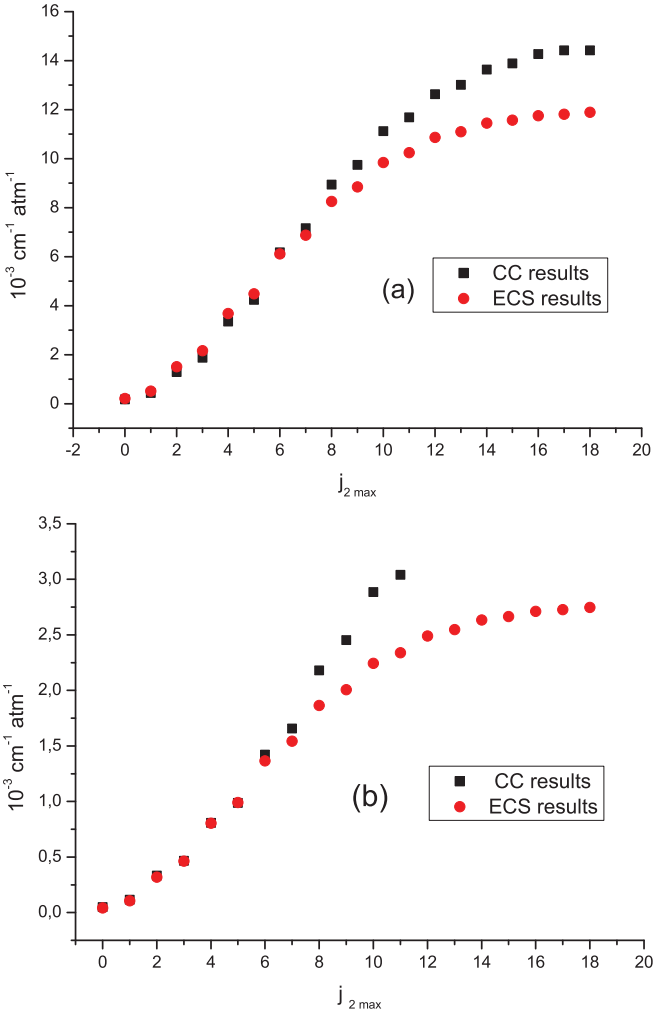

FIG. 2. Convergence of the sum $\sigma\left(j_1 \rightarrow j'_1; T\right) = \sum_{j_2=0}^{j_{2\max}} \rho(j_2)$ $\sum_{j'_2} \sigma\left(j_1, j_2 \rightarrow j'_1, j'_2; T\right)$ as function of $j_{2\max}$: (a) for $j_1 = 4$, $j'_1 = 6$ and (b) for $j_1 = 14, j'_1 = 16$.

benchmark CC/CS values. As a consequence, the linewidth cross section $\sigma^0(14, 14; T = 298\,\text{K})$ as deduced from the sum rule (Eq. (4b)) cannot be labeled as a CC/CS result.

C. Comparison with experimental data

As mentioned previously, rotational excitation rates for $N_2(v = 1)$-$N_2(v = 0)$ collisions have been measured by Sitz and Farrow[19] at 298 K by a pump-probe technique and may be used to check the consistency of our final results. Indeed as shown by Huo and Green,[11] rotational collisional rates do not strongly depend on the different vibrational states of the two colliding partners. As can be seen from Table III, there is a good agreement overall between experiment and theory: most of our CC/CS final results are inside or very close to the error bars of the experimental data. Unfortunately, there are large uncertainties on some of the experimental results and further experimental investigation would be of great interest before any new analysis of the remaining discrepancy between theory and experiment. As outlined previously,[11,14] some of the differences may be due to inaccuracy in the PES and/or to the neglect of exchange contributions. While interesting, such problems are beyond the scope of the present paper. Table IV summarizes the main result of the present work: the fully quantum relaxation matrix at room temperature for the isotropic Raman Q branch of N_2. Note that the diagonal elements are those of Ref. 9. Indeed, since the rule in the present work is to only consider "quite pure CC/CS results" it is not possible to obtain fully converged linewidths from Eq. (4b) for all $Q(j_1)$ lines. The convergence of the diagonal elements was considered in a different way in Ref. 9, by summing first over the post-collisional rotational quantum numbers (j'_1, j'_2), analyzing at that step the convergence and performing then the thermal average and finally summing over j_2 the partial pressure broadening cross-sections $\sigma(j_1, j_2; T)$ weighted by the populations $\rho(j_2)$. Nevertheless, the collisional halfwidths obtained summing the off-diagonal elements of Table IV (Eq. (4b)) reproduce the main trend with j_1 of the diagonal elements[9] and lead to very close values to the latter at least for the first few values. Due to the lack of off-diagonal terms for $j_1(j'_1) > 12$ the agreement strongly deteriorates for $j_1 > 10$.

TABLE III. One body rate constants for $j_1 \rightarrow j'_1$ transitions at 298 K, in μs^{-1} $Torr^{-1}$. Comparison of our CC/CS results, completed by ECS corrections, with the experimental data of Sitz and Farrow.[19]

j_1	j'_1	Experiment	CC/CS final results
0	2	6.64 ± 1.18	7.23
0	4	3.76 ± 0.83	3.78
0	6	2.73 ± 0.61	2.58
0	8	0.86 ± 0.51	1.69
0	10	0.64 ± 0.12	0.94
0	12	0.29 ± 0.06	0.45
0	14	0.22 ± 0.04	0.175
2	4	5.13 ± 0.58	4.52
2	6	2.40 ± 0.44	2.83
2	8	1.52 ± 0.34	1.81
2	10	0.97 ± 0.22	1.01
2	12	0.28 ± 0.14	0.49
2	14	0.12 ± 0.04	0.19
4	6	4.7 ± 0.6	3.74
4	8	2.2 ± 0.4	2.12
4	10	1.4 ± 0.2	1.15
4	12	0.54 ± 0.13	0.56
4	14	0.21 ± 0.04	0.22
6	8	3.37 ± 0.47	3.18
6	10	2.22 ± 0.29	1.51
6	12	0.71 ± 0.14	0.77
6	14	0.23 ± 0.05	0.28
8	10	2.52 ± 0.41	2.65
8	12	1.12 ± 0.22	1.07
8	14	0.29 ± 0.07	0.39
10	12	2.68 ± 0.43	2.26
10	14	1.04 ± 0.13	0.72
12	14	1.83 ± 0.26	1.96

TABLE IV. CC/CS relaxation matrix W for N_2-N_2 at 298 K (The $W_{j',j}$ elements are expressed in 10^{-3} cm^{-1} atm^{-1}). Diagonal elements have been reported in Ref. 9.

j / j'	0	2	4	6	8	10	12	14
0	68.2	− 6.2	− 2.1	− 1.22	− 0.82	− 0.54	− 0.34	− 0.185
2	− 29.2	50.3	− 11.6	− 6.3	− 4.1	− 2.7	− 1.69	− 0.966
4	− 15.3	− 18.3	46.0	− 13.0	− 7.53	− 4.8	− 3.05	− 1.745
6	− 10.46	− 11.5	− 15.1	44.4	− 13.14	− 7.3	− 4.9	− 2.575
8	− 6.84	− 7.33	− 8.6	− 12.9	44.0	− 12.57	− 6.67	− 3.59
10	− 3.81	− 4.1	− 4.67	− 6.12	− 10.73	42.3	− 11.8	− 5.5
12	− 1.84	− 1.97	− 2.26	− 3.13	− 4.34	− 9.13	40.1	− 11.37
14	− 0.7	− 0.77	− 0.88	− 1.13	− 1.6	− 2.9	− 7.92	34.1

IV. CONCLUSION

To summarize, using the most recent rigid rotor N_2-N_2 potential reported so far, we have carried out, at the CC and CS levels, room temperature calculations of the relaxation matrix for the isotropic Raman Q branch of N_2. Such a temperature gives rise numerical problems associated with the convergence of the quantum calculations. However, we have shown that it is possible to quantify the convergence by using the ECS approximation. We then demonstrated that for moderate values of the rotational quantum number $j \leq 12$, the convergence of our CC/CS cross sections has been practically achieved, since ECS complements are limited to a few percent. This fully quantum relaxation matrix is expected to be a benchmark for testing the validity of more approximate methods using the same PES, in particular the semi-classical approach proposed in Ref. 6.

[1] J. M. Hartmann, C. Boulet, and D. Robert, *Collisional Effects on Molecular Spectra. Laboratory Experiments and Models, Consequences for Applications* (Elsevier, Amsterdam, 2008).
[2] S. Green, J. Chem. Phys. **62**, 2271 (1975).
[3] R. G. Gordon, J. Chem. Phys. **46**, 448 (1967); R. G. Gordon and R. P. McGinnis, *ibid.* **55**, 4898 (1971).
[4] W. B. Neilsen and R. G. Gordon, J. Chem. Phys. **58**, 4131 (1973).
[5] K. S. Lam, J. Quant. Spectrosc. Radiat. Transf. **17**, 351 (1977).
[6] Q. Ma, C. Boulet, and R. H. Tipping, J. Chem. Phys. **139**, 034305 (2013).
[7] D. Robert and J. Bonamy, J. Phys. **40**, 923 (1979).
[8] F. Thibault, R. Z. Martinez, D. Bermejo, and L. Gomez, J. Quant. Spectrosc. Radiat. Transf. **112**, 2542 (2011).
[9] F. Thibault, L. Gomez, S. V. Ivanov, O. G. Buzykin, and C. Boulet, J. Quant. Spectrosc. Radiat. Transf. **113**, 1887 (2012).
[10] L. Gomez, B. Bussery-Honvault, T. Cauchy, M. Bartolomei, D. Cappelletti, and F. Pirani, Chem. Phys. Lett. **445**, 99 (2007); D. Cappelletti, F. Pirani, B. Bussery-Honvault, L. Gomez, and M. Bartolomei, Phys. Chem. Chem. Phys. **10**, 4281 (2008).
[11] (a) W. H. Huo and S. Green, J. Chem. Phys. **104**, 7572 (1996); (b) S. Green and W. H. Huo, *ibid.* **104**, 7590 (1996).
[12] A. van der Avoird, P. E. S. Wormer, and A. P. J. Jansen, J. Chem. Phys. **84**, 1629 (1986).
[13] D. Cappelletti, F. Vechiocattivi, F. Pirani, E. L. Heck, and A. S. Dickinson, Mol. Phys. **93**, 485 (1998).
[14] J. P. Fonfria, A. Ramos, F. Thibault, G. Tejeda, J. M. Fernandez, and S. Montero, J. Chem. Phys. **127**, 134305 (2007).
[15] A. Ben-Reuven, Phys. Rev. **141**, 34 (1966).
[16] S. Green, J. Chem. Phys. **98**, 257 (1993).
[17] M. H. Karimi-Jafari and M. Ashouri, Phys. Chem. Chem. Phys. **13**, 9887 (2011).
[18] J. M. Hutson and S. Green, MOLSCAT version 14, Collaborative Computational Project 6 of the UK Science and Engineering Research Council, UK, 1995. George C. McBane, "PMP Molscat," a parallel version of Molscat version 14, Grand Valley State University, 2005, see http://faculty.gvsu.edu/mcbaneg/pmpmolscat.
[19] G. O. Sitz and R. L. Farrow, J. Chem. Phys. **93**, 7883 (1990).
[20] A. E. DePristo, S. D. Augustin, R. Ramaswamy, and H. Rabitz, J. Chem. Phys. **71**, 850 (1979).